



This is an *Accepted Manuscript*, which has been through the RSC Publishing peer review process and has been accepted for publication.

Accepted Manuscripts are published online shortly after acceptance, which is prior to technical editing, formatting and proof reading. This free service from RSC Publishing allows authors to make their results available to the community, in citable form, before publication of the edited article. This *Accepted Manuscript* will be replaced by the edited and formatted *Advance Article* as soon as this is available.

To cite this manuscript please use its permanent Digital Object Identifier (DOI®), which is identical for all formats of publication.

More information about *Accepted Manuscripts* can be found in the [Information for Authors](#).

Please note that technical editing may introduce minor changes to the text and/or graphics contained in the manuscript submitted by the author(s) which may alter content, and that the standard [Terms & Conditions](#) and the [ethical guidelines](#) that apply to the journal are still applicable. In no event shall the RSC be held responsible for any errors or omissions in these *Accepted Manuscript* manuscripts or any consequences arising from the use of any information contained in them.

Graphic abstract

Aggregation-induced emission of triphenylamine substituted cyanostyrene derivatives



New triphenylamine substituted cyanostyrene luminogens (G1, G1-N and G2) with aggregation-induced emission (AIE) were synthesized.

Cite this: DOI: 10.1039/c0xx00000x

www.rsc.org/xxxxxx

PAPER

Aggregation-induced emission of triphenylamine substituted cyanostyrene derivatives†

Xin Zhao^a, Pengchong Xue^a, Kai Wang^a, Peng Chen^b, Peng Zhang^a, Ran Lu^{a,*}

Received (in XXX, XXX) Xth XXXXXXXXXX 20XX, Accepted Xth XXXXXXXXXX 20XX

DOI: 10.1039/b000000x

Cyanostyrene-based D- π -A type conjugated compounds bearing triphenylamine units (**G1**, **G1-N** and **G2**) have been synthesized. By tuning the conjugated skeleton and the withdrawing electron ability of the acceptor, green, orange and red light emitters were achieved. It is interesting that although their emissions in solutions were weak, we observed strong emission in solid states. For example, the Φ_F of the dendritic molecule **G2** in power reached 0.67, which was more than 20 times of that in THF. The single crystal X-ray diffraction data revealed that the intermolecular H-bonds of C-H \cdots O, C-H \cdots N and C-H \cdots π led to the increased rigidity of the molecular skeleton, which would restrict the intramolecular rotation, yielding high Φ_F in solid states. These AIE compounds may become candidates for emitting materials.

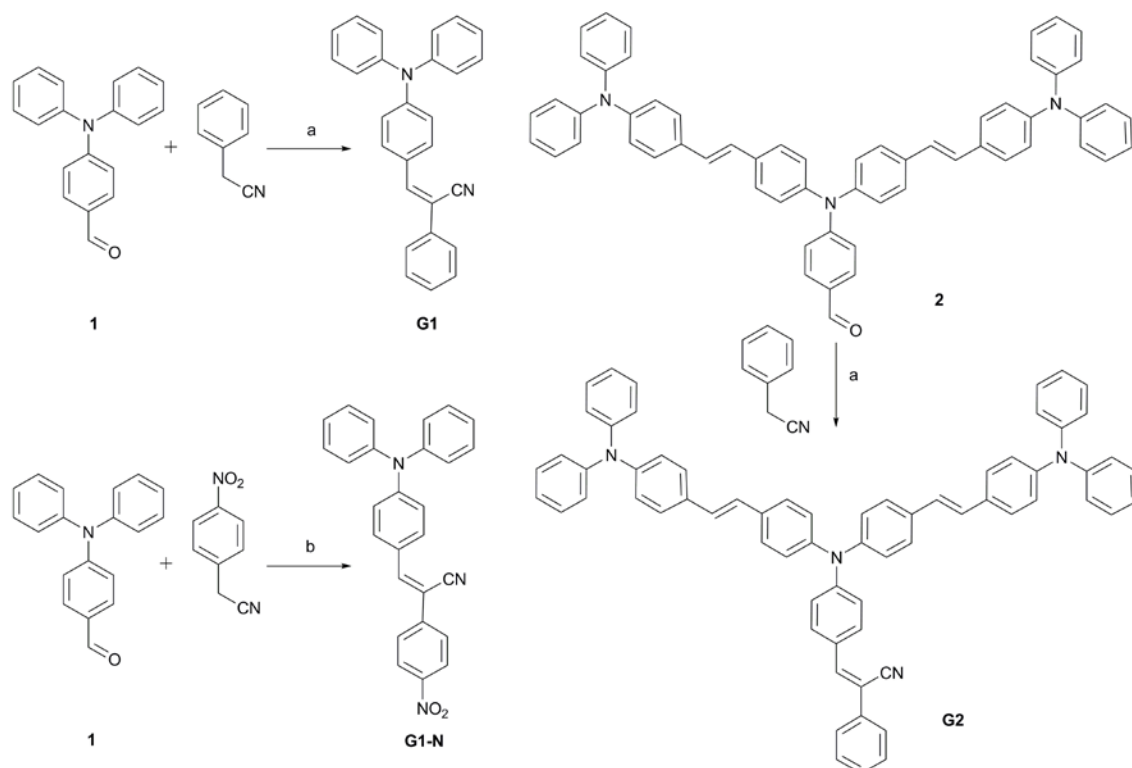
Introduction

Organic π -conjugated molecules have been intensively studied due to their potential applications in opto-electronic materials.¹⁻⁵ Most of organic luminogens are highly emissive in dilute solutions but exhibit weak or quenching fluorescence upon increasing the concentrations of the solutions or in the solid states because of strong π - π interactions and non-radiative decay process. This phenomenon, which is known as aggregation-caused quenching (ACQ),⁶⁻⁷ has greatly limited the practical applications. Numerous efforts have been made to tackle this problem,⁸⁻⁹ and the most important development in this field was the introduction of the term of aggregation-induced emission (AIE) by Tang and co-workers in 2001.¹⁰ They found that 1-methyl-1,2,3,4,5-pentaphenylsilole gave very weak emission in solution, but the obtained nanoparticles could emit strong fluorescence because of restriction of intramolecular rotation (RIR). Additionally, Park reported that 1-cyano-*trans*-1,2-bis-(4'-methylbiphenyl)-ethylene (CN-MBE) was non-luminescent in solution but highly emissive in the aggregated states.¹¹⁻¹²

Because the achievement of the emitting materials with strong emission in solid states is important in their applications in OLEDs, laser devices, and so on, various conjugated organic molecules emitting different colors have been synthesized.¹³ For example, the oligofluorenes were linked to different cores, such as porphyrin and tetraphenylsilica, to give red and blue emission in OLEDs, respectively.¹⁴⁻¹⁵ The trimer of tetraphenylethene (TPE) gave a fluorescence peak at 494 nm, which shifted to 575 nm when fumaronitrile was used as a center linked to TPE units. In addition, an emission at 713 nm was achieved in fumaronitrile-centered TPE bearing terminal N,N-diethylamino group.¹⁶ Tian and coworkers designed a series of 2,2'-biindene-based fluorophores with strong solid-state emissions ranged from deep blue to red, which were tuned by the variation of the substituents

on the 2,2'-biindanyl unit or by adjustment of the aggregation state.¹⁷ Moreover, the luminogens emitting blue, green, and red colors constructed from tetraphenylethene, benzo-2,1,3-thiadiazole and thiophene were prepared.^{18,19} It is known that triphenylamine (TPA) has been widely used as the electron donor (D) in opto-electronic materials on account of its good hole transport mobility²⁰⁻²² and the cyanostyrene is a typical electron acceptor (A) group with AIE activity.²³⁻²⁵ Recently, Tian found that the multi-branched D- π -A- π -D compounds using triphenylamine (or carbazole) group as electron-donor, cyanostyrene (or triazine) group as electron-acceptor showed excellent two-photon absorption activity and AIE properties.²⁶

Herein, in order to prepare new AIE materials emitting different colors we designed D- π -A conjugated compounds bearing TPA and cyanostyrene units **G1**, **G1-N** and **G2** (Scheme 1). Although their emission in solutions was weak, we observed strong emission in green, orange and red in solid states, which were tuned by the conjugated length and the withdrawing electron ability of the acceptor. For example, the second generation of triphenylamine-based dendron was involved in **G2**²⁷⁻²⁹ leading to larger conjugation than that of **G1**, so **G2** emitted orange light and **G1** emitted green light in solid states. When nitro group was introduced to cyanostyrene unit, red emitting compound **G1-N** was obtained.³⁰ The single crystal X-ray diffraction data revealed that the intermolecular H-bonds of C-H \cdots O, C-H \cdots N and C-H \cdots π led to the increasing rigidity of molecular skeleton, which would restrict the intramolecular rotation, yielding high Φ_F in solid states. Therefore, green, orange and red emitting compounds with AIE were obtained, which might have potential applications in organic light emitting materials.



Scheme 1 Synthetic routes for **G1**, **G1-N** and **G2**.

Results and discussion

Syntheses

The synthetic routes for triphenylamine substituted cyanostyrene derivatives are described in **Scheme 1**. Firstly, the formyl-ended triphenylamine derivatives **1** and **2** were prepared according to the methods reported by our group previously.³¹ The Knoevenagel condensation reaction between formyl-ended triphenylamine derivative (compound **1** or **2**) and phenylacetonitrile catalyzed by sodium hydroxide afforded **G1**³² and **G2** in yield of 85% and 79%, respectively. Similarly, the Knoevenagel condensation reaction between compound **1** and 2-(4-nitrophenyl)acetonitrile catalyzed by tetrabutylammonium hydroxide (TBAH) gave **G1-N** in a yield of 90 %. All the new compounds were characterized with FT-IR, ¹H NMR, ¹³C NMR and MALDI/TOF mass spectroscopy, and they are soluble in dichloromethane, chloroform and THF. From the FT-IR spectra for **G2** we found the vibration absorption band appeared at ca. 960 cm⁻¹, meaning that the carbon-carbon double bonds adopted in *trans*-forms. In addition, the ¹H NMR spectra of **G2** further confirmed that ethenyl groups adopted the *trans*-conformation on account of the absence of the signal at ca. 6.5 ppm assigned to the protons in *cis*-double bonds.³¹

UV-vis absorption and fluorescence emission spectra

The UV-vis absorption and fluorescence emission spectra of triphenylamine substituted cyanostyrene derivatives **G1**, **G1-N** and **G2** in THF (1.0×10⁻⁵ M) were shown in **Figure 1a** and the

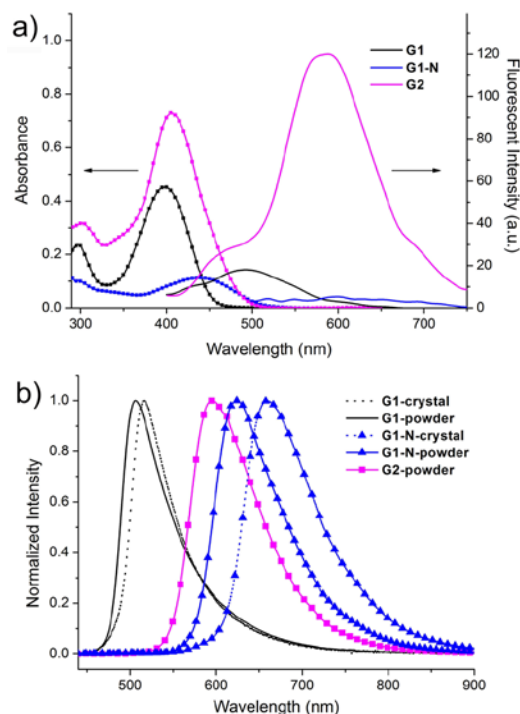
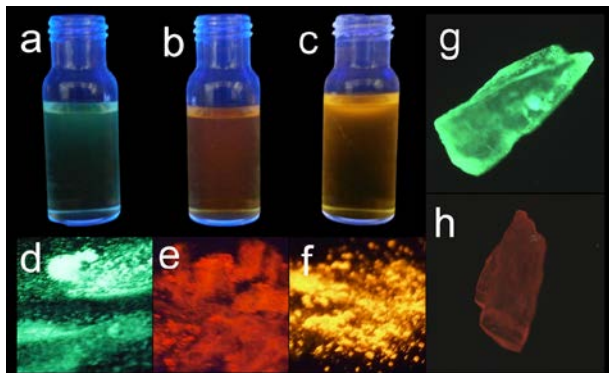


Fig. 1 a) UV-vis absorption and fluorescence emission ($\lambda_{\text{ex}} = 365 \text{ nm}$) spectra of **G1**, **G1-N** and **G2** in THF ($1.0 \times 10^{-5} \text{ M}$); b) Fluorescence emission spectra of **G1**, **G1-N** and **G2** in solid states ($\lambda_{\text{ex}} = 365 \text{ nm}$).

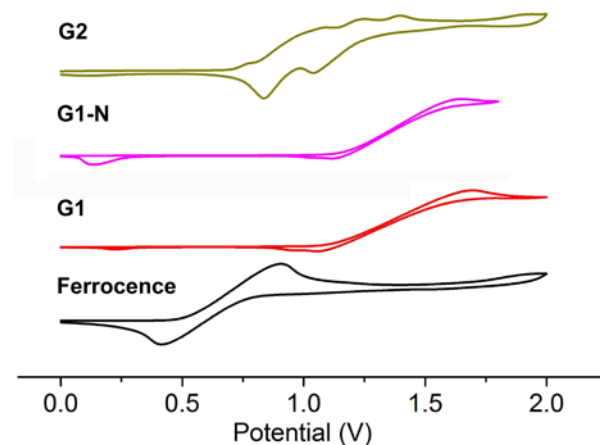
Table 1 UV-vis absorption and fluorescence data of triphenylamine derivatives.

Molecule	Solution			Powder		Crystal	
	$\lambda_{\text{abs}}/\text{nm}$	$\lambda_{\text{em}}/\text{nm}^a$	Φ_F^b	$\lambda_{\text{em}}/\text{nm}^a$	Φ_F^c	$\lambda_{\text{em}}/\text{nm}^a$	Φ_F^c
G1	298, 398	494	0.02	506	0.33	516	0.31
G1-N	439	- ^d	0.01	624	0.09	658	0.06
G2	303, 406	584	0.03	596	0.67	- ^d	- ^d

^a Excited at 365 nm.^b Quantum yields (Φ_F) determined in THF using an integrating sphere.^c Quantum yields (Φ_F) determined using an integrating sphere.^d Not obtained.**Fig. 2** Photos of **G1**, **G1-N** and **G2** in THF (a, b and c, respectively) and in powders (d, e and f, respectively) under UV illumination (365 nm), and fluorescent microscopy ($\lambda_{\text{ex}}=330-385$ nm) images of **G1** (g) and **G1-N** (h) in crystals.

corresponding photophysical data are presented in **Table 1**. Two clear absorption peaks at ca. 300 nm and 400 nm were detected for compounds **G1** and **G2**. The former one can be attributed to the $\pi-\pi^*$ transition of triphenylamine group and the latter one can be assigned to the intramolecular charge transfer (ICT) band. In detail, the absorption bands of **G1** were located at 298 nm and 398 nm, which red-shifted to 303 nm and 406 nm for **G2** due to the enlarged conjugation of the increased dendritic structure. On account of the introduction of nitro group the maximum absorption of **G1-N** red-shifted to 439 nm, and its absorption intensity was quite lower than that of **G1** due to the spin-forbidden charge transfer.³³ It is notable that the intensities of the absorption peaks for **G2** was higher than **G1** and **G1-N** due to the increased number of vinyl triphenylamine units in **G2**. From the fluorescence emission spectra of **G1**, **G1-N** and **G2** in THF we can find that **G1-N** was almost non-emissive because the introduction of electron withdrawing group of nitro into cyanostyrene unit might lead to the occurrence of photo-induced electron transfer from triphenylamine to the acceptor. **G1** gave a weak emission at 494 nm. With increasing the generation of the dendron based on triphenylamine, a red-shift of emission band located at 584 nm was observed for **G2** due to the larger π -conjugation. The fluorescent quantum yields (Φ_F) of **G1**, **G1-N** and **G2** in THF were 0.02, 0.01 and 0.03 using an integrating sphere, meaning that the emission was very weak.

The fluorescence emission spectra of **G1**, **G1-N** and **G2** in powders or in crystals were shown in **Figure 1b**. It was found

**Fig. 3** Cyclic voltammograms of **G1**, **G1-N** and **G2** in CH_2Cl_2 containing 0.1 mol L^{-1} of tetrabutylammonium tetrafluoroborate (TBABF_4)

that the emission of **G1** and **G2** in powders appeared at 506 nm and 596 nm, respectively, with a red-shift compared with those in solutions due to the aggregation. Although **G1-N** was non-emissive in solution, its powder gave an obvious emission at 652 nm. Notably, the Φ_F values for these compounds in powders were more than 20 times of those in solutions (**Table 1**), indicating they exhibited AIE properties. Moreover, the crystals of **G1** and **G1-N** (the crystal of **G2** was not obtained) also gave strong emission, and their emission bands further red-shifted to 516 nm and 658 nm in the crystals. The Φ_F values for **G1** and **G1-N** in crystals were 0.31 and 0.06, respectively, which were similar to those in powders. In addition, the photos of **G1**, **G1-N** and **G2** in solutions and in solid states illuminated by UV light as shown in **Figure 2** further illustrated that the emission was enhanced significantly in powders as well as in crystals compared with that in solutions.

Electrochemical properties

The electrochemical behaviors of triphenylamine substituted cyanostyrene derivatives were investigated by cyclic voltammetry (CV) using a standard three-electrode cell and an electrochemical workstation (CHI 604) under N_2 atmosphere. **Figure 3** showed the cyclic voltammetry (CV) diagrams of **G1**, **G1-N** and **G2** using 0.1 M tetrabutylammonium tetrafluoroborate (TBABF_4) as supporting electrolyte in dry CH_2Cl_2 , with a glass carbon disc working electrodes, a platinum-wire counter electrode, and an SCE reference electrode. The SCE reference electrode was calibrated using the ferrocene/ferrocenium (Fc/Fc^+) redox couple as an external standard. According to the redox potential of Fc/Fc^+ (with an absolute energy level of -4.8 eV relative to the vacuum level for calibration), the HOMO energy level was calculated to be -5.52 eV for **G1**, -5.52 eV for **G1-N** and -4.91 eV for **G2** (**Table S1**), respectively. The higher HOMO energy level of **G2** indicated its strong electron donating ability. The calculated LUMO energy level for **G1-N** (-3.10 eV) was lower than that of **G1** (-2.78 eV) and **G1** (-2.35 eV) due to the strong accepting ability of the nitro group.

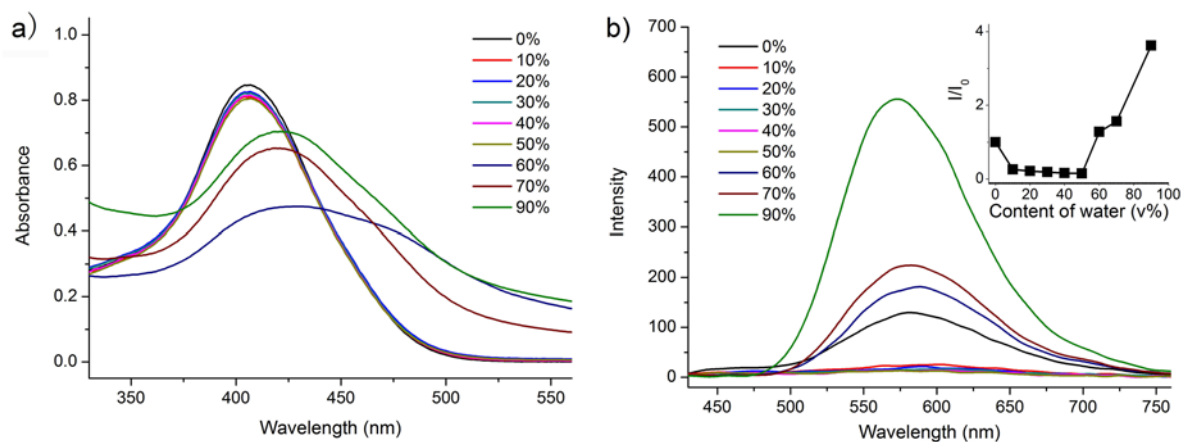


Fig. 4 a) UV-vis absorption and b) fluorescence emission spectra ($\lambda_{\text{ex}} = 365$ nm) of **G2** (1.0×10^{-5} M) in THF/water with different amount of water (% volume). Inset of b) plots of PL integral versus water content of the solvent mixture for **G2**.

5 AIE properties

As discussed above, compounds **G1**, **G1-N** and **G2** exhibited AIE behaviors. In order to evaluate the AIE properties of these compounds, **G2** was selected as an example. The UV-vis absorption and fluorescence emission spectral changes of **G2** in the THF/water (**G2** is soluble in THF and water is a poor solvent) with different amount of water were given in **Figure 4**. It was found that when the amount of water was ≤ 50 % (volume content) the UV-vis absorption spectra of **G2** were similar to that in pure THF. Upon further increasing of the amount of water, the absorption band at 406 nm red-shifted and was broadened, which might be due to the molecular aggregation.²³ For example, the absorption red-shifted to 420 nm and 422 nm when the contents of water were 70 % and 90 % in THF/water, respectively. In addition, the appearance of tails in the visible region could be attributed to Mie scattering caused by nanoparticles.¹¹ From **Figure 4b**, we could find that the emission of **G2** can hardly be detected when the volume content of water was ≤ 50 % in THF/water. However, with further increasing the amount of water in the system, the fluorescence emission of **G2** was enhanced significantly, accompanied with a blue-shift. The emission appeared at 582 nm and 573 nm when the volume contents of water were 70 % and 90 % in THF/water, respectively. In addition, we presented the plot of the ratio of I/I_0 , in which I was the integral of fluorescence emission in the mixed solvent and I_0 was that in pure THF, vs the content of water in THF/water. As shown in inset of **Figure 4b**, when the volume content of water was ≤ 50 %, I/I_0 values were quite low. With increasing the content of water, I/I_0 values increased significantly, suggesting AIE happened in the aggregates of **G2**.

35 X-ray studies of the single crystals

In order to reveal the mechanism of the AIE phenomena, we tried to get single crystals for all compounds. The crystals of **G1** and **G1-N** were obtained from the solutions in petroleum ether/chloroform, but we could not get the crystal of **G2**. The single crystal study revealed that the crystal structures of **G1** and **G1-N** belonged to the monoclinic space group $P2(1)/n$ and monoclinic space group $P2_1/c$, respectively, and each cell

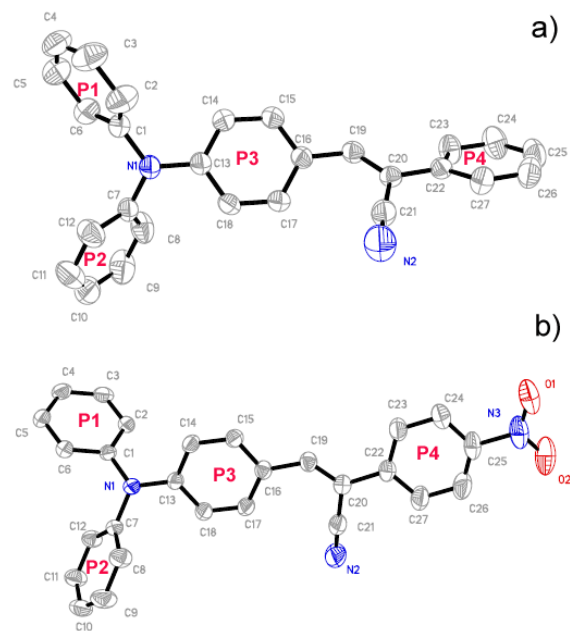


Fig. 5 ORTEP drawings of **G1** (a) and **G1-N** (b) at 50% probability level ellipsoids.

contained four molecules ($Z = 4$). The molecular ORTEP drawings were displayed in **Figure 5**. In the crystal of **G1**, the torsion angle between phenyl rings P3 and P4 was $56.78(21)^\circ$, exhibiting more twisting structure of cyanostyrene than that in **G1-N** ($8.38(6)^\circ$). The twisting structures between two phenyl rings in **G1** reduce the conjugation of molecules and prevent face-to-face π - π aggregations. Moreover, the intermolecular interactions among molecules **G1** were shown in **Figure 6a**. It was found that the H-bond (2.44 \AA) between N (in C-N triple bond) and vinyl-H atom in two adjacent molecules was formed along the short axis of the molecule. The $C24-H \cdots \pi$ (P3) (2.87 \AA) and $C4-H \cdots \pi$ (P3) (2.93 \AA) provided two kinds of interactions for each P3 ring. These C-H \cdots N and C-H \cdots π interactions resulted in a rigid three-dimensional network. Thus, the twisting structure (torsion angle between P3 and P4) and the existence of multiple C-H \cdots π H-bonds restricted the intramolecular rotation and

enabled the molecule to emit light intensively in the solid states.³⁴ In the crystal of **G1-N** (Figure 6b-c), the rings of P3 and P4 were almost coplanar (torsion angle 8.38(6)°) and four kinds of H-bonds were formed. C18-H...N2 (2.58 Å) and C24-H...O1 (2.62 Å) linked the molecules in each layer together along the P3 and P4 plane. Each H-bond of C2-H...O1 (2.60 Å) connected one pair of molecules in adjacent layers, and the H-bond of C5-H...O2 (2.65 Å) provided a head-to-tail type connection. Meanwhile, the C-H... π interactions of 2.61 and 2.93 Å happened between parallel non-planar molecules. Accordingly, RIR process caused by the intermolecular interactions, including C-H... π , C-H...N and C-H...O, resulted in the increased rigidity of molecular skeleton to yield higher Φ_F in crystals than those in solutions.

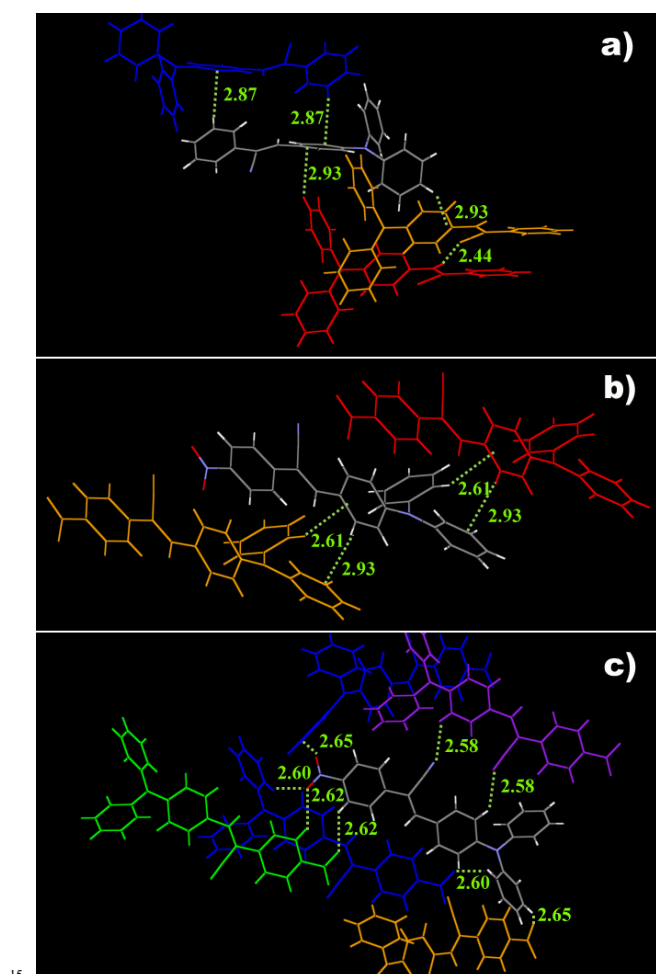


Fig. 6 Intermolecular H-bonds (C-H...O, C-H...N and C-H... π) in the crystals of **G1** (a) and **G1-N** (b, c).

Conclusions

In conclusion, cyanostyrene-based D- π -A conjugated compounds bearing triphenylamine units (**G1**, **G1-N** and **G2**) have been synthesized. By tuning the conjugated skeleton and the withdrawing electron ability of the acceptor, green, orange and red light emitters were achieved. It is interesting that although their emissions in solutions were weak, we observed strong emissions in solid states. For example, the Φ_F of dendritic molecule **G2** in power reached 0.67, which was more than 20

times of that in THF. The single crystal X-ray diffraction data revealed that the intermolecular H-bonds of C-H...O, C-H...N and C-H... π led to the increased rigidity of the molecular skeleton, which would restrict the intramolecular rotation, yielding high Φ_F in solid states. Therefore, the green, orange and red emitting compounds with AIE properties were obtained, which might have potential applications in organic light emitting materials.

Experimental Section

General

Solvents were purified and dried using standard protocols. All other chemical reagents were obtained commercially and were used as received without further purification. ¹H NMR spectra were recorded on a mercury plus 400 MHz using CDCl₃ as solvent in all cases. ¹³C NMR spectra were recorded on a mercury plus 100 MHz using CDCl₃ as solvent. FT-IR spectra were measured using a Germany Bruker Vertex 80v FT-IR spectrometer by incorporating samples in KBr disks. Mass spectra were performed on Agilent 1100 MS series and AXIMA CFR MALDI/TOF (Matrix assisted laser desorption ionization/Time-of-flight) MS (COMPACT). UV-vis absorption spectra were determined on a Shimadzu UV-1601PC spectrophotometer. Fluorescence emission spectra were carried out on a Shimadzu RF-5301 luminescence spectrometer. The emission spectra of solids were recorded using Maya2000 Pro CCD spectrometer. The absolute fluorescence quantum yields were measured on Edinburgh FLS920 steady state fluorimeter. The fluorescence microscopy images were obtained from Olympus BX51 fluorescence microscopy. Cyclic voltammetry was carried out with a CHI 604B electrochemical working station at room temperature at a scan rate of 50 mV/s.

Synthetic procedures and characterizations

(Z)-3-(4-(diphenylamino)phenyl)-2-phenylacrylonitrile (**G1**)

A mixture of formyl-ended triphenylamine derivative **1** (0.6 mmol), phenylacetonitrile (0.9 mmol), and sodium hydroxide (0.9 mmol) in ethanol (50 mL) was stirred for 24 h at room temperature under an atmosphere of nitrogen. Then, the precipitate was filtered off, washed with cold ethanol. Yield: 85%. M.p. 148.0-151.0 °C. ¹H NMR (400 MHz, CDCl₃) δ 7.774 (d, J = 8 Hz, 2H), 7.642 (d, J = 8 Hz, 2H), 7.402-7.440 (m, 3H), 7.294-7.365 (m, 5H), 7.100-7.168 (m, 6H), 7.048 (d, J = 8 Hz, 2H) (Figure S1). ¹³C NMR (100 MHz, CDCl₃) δ 149.98, 146.66, 141.73, 135.08, 130.69, 129.61, 129.02, 128.60, 126.50, 125.73, 124.41, 120.96, 118.79, 107.80 (Figure S2). FT-IR (KBr, cm⁻¹): 2216, 1583, 1506, 1489, 1448, 1329, 1298, 1275, 1192, 1178, 831, 760, 696. MS, m/z: cal: 372.16, found: 372.9 (Figure S3).

(Z)-3-(4-(diphenylamino)phenyl)-2-(4-nitrophenyl)acrylonitrile(**G1-N**)

A mixture of 4-(diphenylamino)benzaldehyde (0.16g, 0.6 mmol), phenylacetonitrile (0.1g, 0.9 mmol), and tetrabutylammonium hydroxide (TBAH) (0.13g, 0.9 mmol) in ethanol (50 mL) was refluxed for 12 h under an atmosphere of nitrogen. After cooled down to room temperature, the precipitate was filtered off, washed with cold ethanol to give a red solid. Yield: 90%. M.p. 160.0-162.0 °C. ¹H NMR (400 MHz, CDCl₃) δ 8.272 (d, J = 8 Hz, 2H), 7.784-7.832 (m, 4H), 7.548 (s, 1H), 7.324-7.361 (m,

4H), 7.147-7.190 (m, 6H), 7.038 (d, $J = 8$ Hz, 2H) (**Figure S4**). ^{13}C NMR (100 MHz, CDCl_3) δ 151.08, 147.24, 146.14, 144.76, 141.45, 131.50, 129.74, 126.15, 126.10, 125.13, 125.04, 124.31, 120.00, 118.11, 104.60 (**Figure S5**). FT-IR (KBr, cm^{-1}): 2218, 1574, 1514, 1485, 1340, 1284, 1198, 1180, 849, 752. MS, m/z : cal: 417.15, found: 417.2 (**Figure S6**).

(Z)-3-(4-(bis(4-(diphenylamino)styryl)phenyl)amino)phenyl)-2-phenylacrylonitrile (G2)

G2 was prepared from formyl-ended triphenylamine derivative **2** and phenylacetonitrile by using similar procedure for **G1**. The crude product was purified by column chromatography (silica gel) using dichloromethane as elute. Yield: 85%. M.p. 112.0-116.0 °C. ^1H NMR (400 MHz, CDCl_3) δ 7.835 (d, $J = 8$ Hz, 2H), 7.686 (m, $J = 8$ Hz, 2H), 7.370-7.476 (m, 13H), 7.275-7.312 (m, 5H), 7.137-7.176 (m, 14H), 6.976-7.092 (m, 14H) (**Figure S7**). ^{13}C NMR (100 MHz, CDCl_3) δ 149.43, 147.57, 147.32, 145.51, 141.58, 135.03, 133.79, 131.59, 130.72, 129.31, 129.02, 128.66, 127.65, 127.45, 127.31, 127.04, 126.23, 125.76, 125.47, 124.52, 123.62, 123.06, 121.71, 118.72, 108.12, 77.37, 77.06, 76.74 (**Figure S8**). FT-IR (KBr, cm^{-1}): 2204, 1589, 1508, 1490, 1325, 1281, 1178, 960, 829, 754. MS, m/z : cal: 910.4, found: 912.4 (**Figure S9**).

X-ray crystal structure determination

Diffraction data of single crystals were collected on a Rigaku RAXIS-PRID diffractometer using the ω -scan mode with graphite-monochromator $\text{Mo-K}\alpha$ radiation. The structure was solved with direct methods using the SHELXTL programs and refined with full-matrix least-squares on F^2 .³⁵ The corresponding CCDC reference number (CCDC: 968916 for **G1** and CCDC: 968917 for **G1-N**) and the data can be obtained free of charge from The Cambridge Crystallographic Data Centre via www.ccdc.cam.ac.uk/data_request/cif.

Table 2 Crystal data for **G1** and **G1-N**.

Compound	G1	G2
Empirical formula	$\text{C}_{27}\text{H}_{20}\text{N}_2$	$\text{C}_{27}\text{H}_{19}\text{N}_3\text{O}_2$
Formula wt	372.45	417.45
Temperature, K	293(2) K	293(2) K
Crystal system	monoclinic	monoclinic
Space group	P2(1)/n	P2 ₁ /c
<i>a</i> , Å	17.164(3)	11.154(2)
<i>b</i> , Å	6.6995(13)	7.5463(15)
<i>c</i> , Å	19.809(4)	25.707(5)
α /°	90.00	90.00
β /°	111.08(3)	96.42(3)
γ /°	90.00	90.00
Volume, Å ³	2125.4(7)	2150.3(7)
<i>Z</i>	4	4
density, Mg m ⁻³	1.164	1.289
μ (Mo K α), mm ⁻¹	0.068	0.083
θ range, deg	3.09 – 27.48	3.14 – 27.48
no. of reflns collected	19408	19989
no. of unique reflns	4844	4896
<i>R</i> (int)	0.0598	0.0507
GOF	0.982	1.031
<i>R</i> 1 [$I > 2\sigma(I)$]	0.0535	0.0542
<i>wR</i> 2 [$I > 2\sigma(I)$]	0.1219	0.1212
<i>R</i> 1 (all data)	0.1192	0.1153
<i>wR</i> 2 (all data)	0.1451	0.1423

Preparation of aggregates for AIE measurement

The solution of **G2** in THF was firstly prepared (1.0×10^{-5} M). Then, 1 mL of the above solution was transferred to a volumetric flask (10 mL). After adding an appropriate amount of THF, water was added dropwise under vigorous stirring to furnish a 10 mL solution in a THF/water with a specific water fraction. The water content was varied in the range of 0-90 vol %. The UV-vis absorption and fluorescence emission spectra of the resulting samples were measured immediately after preparation.

Acknowledgements

This work was financially supported by the National Natural Science Foundation of China (51073068, 21374041), the 973 Program (2009CB939701), and the Open Project of the State Key Laboratory of Supramolecular Structure and Materials (SKLSSM201203).

Notes and references

- ^aState Key Laboratory of Supramolecular Structure and Materials, College of Chemistry, Jilin University, Changchun 130012, PR China. Fax: +86-431-88499179; Tel: +86-431-88499179; E-mail: luran@mail.jlu.edu.cn
- ^bKey Laboratory of Functional Inorganic Material Chemistry (MOE), School of Chemistry and Materials Science, Heilongjiang University, Harbin 150080, PR China.
- [†] Electronic Supplementary Information (ESI) available: Electrochemical properties, ^1H -, ^{13}C -NMR spectra and MALDI/TOF MS spectra. See DOI: 10.1039/b000000x/
- P. L. Burn, S.-C. Lo and I. D. W. Samuel, *Adv. Mater.*, 2007, **19**, 1675.
 - J. Liu, Y. Cheng, Z. Xie, Y. Geng, L. Wang, X. Jing and F. Wang, *Adv. Mater.*, 2008, **20**, 1357.
 - C. Li and Z. Bo, *Polymer*, 2010, **51**, 4273.
 - H. Tian and S. Yang, *Chem. Soc. Rev.*, 2004, **33**, 85-97.
 - Y. Hong, J. W. Y. Lam and B. Z. Tang, *Chem. Soc. Rev.*, 2011, **40**, 5361.
 - R. H. Friend, R. W. Gymer, A. B. Holmes, J. H. Burroughes, R. N. Marks, C. Taliani, D. D. C. Bradley, D. A. Dos Santos, J. L. Bredas, M. Logdlund and W. R. Salaneck, *Nature*, 1999, **397**, 121.
 - S. A. Jenekhe and J. A. Osaheni, *Science*, 1994, **265**, 765.
 - S. Hecht and J. M. J. Frechet, *Angew. Chem., Int. Ed.*, 2001, **40**, 74.
 - L. Chen, S. Xu, D. McBranch and D. Whitten, *J. Am. Chem. Soc.*, 2000, **122**, 9302.
 - J. D. Luo, Z. L. Xie, J. W. Y. Lam, L. Cheng, H. Y. Chen, C. F. Qiu, H. S. Kwok, X. W. Zhan, Y. Q. Liu, D. B. Zhu and B. Z. Tang, *Chem. Commun.*, 2001, 1740.
 - B. K. An, S. K. Kwon, S. D. Jung and S. Y. Park, *J. Am. Chem. Soc.*, 2002, **124**, 14410.
 - Z. Zhao, J. W. Y. Lam and B. Z. Tang, *J. Mater. Chem.*, 2012, **22**, 23726.
 - K. E. Sapsford, L. Berti, I. and L. Medintz, *Angew. Chem. Int. Ed.*, 2006, **45**, 4562.
 - B. Li, J. Li, Y. Fu and Z. Bo, *J. Am. Chem. Soc.*, 2004, **126**, 3430.
 - X. Liu, C. He, J. Huang and J. Xu, *Chem. Mater.*, 2005, **17**, 434.
 - X. Y. Shen, Y. J. Wang, E. Zhao, W. Z. Yuan, Y. Liu, P. Lu, A. Qin, Y. Ma, J. Z. Sun, and B. Z. Tang, *J. Phys. Chem. C*, 2013, **117**, 7334.
 - Z. Zhang, B. Xu, J. Su, L. Shen, Y. Xie and H. Tian, *Angew. Chem. Int. Ed.*, 2011, **50**, 11654.
 - Z. Zhao, C. Deng, S. Chen, J. W. Y. Lam, W. Qin, P. Lu, Z. Wang, H. S. Kwok, Y. Ma, H. Qiu and B. Z. Tang, *Chem. Commun.*, 2011, **47**, 8847.
 - Z. Zhao, S. Chen, X. Shen, F. Mahtab, Y. Yu, P. Lu, J. W. Y. Lam, H. S. Kwok and B. Z. Tang, *Chem. Commun.*, 2010, **46**, 686.

- 20 Y. Tao, Q. Wang, Y. Shang, C. Yang, L. Ao, J. Qin, D. Ma and Z. Shuai, *Chem. Commun.*, 2009, 77.
- 21 A. Goel, M. Dixit, S. Chaurasia, A. Kumar, R. Raghunandan, P. R. Maulik and R. S. Anand, *Org. Lett.*, 2008, **10**, 2553.
- 5 22 Z. Ning and H. Tian, *Chem. Commun.*, 2009, 5483.
- 23 S. B. Noh, R. H. Kim, W. J. Kim, S. Kim, K.-S. Lee, N. S. Cho, H.-K. Shim, H. E. Pudavar and P. N. Prasad, *J. Mater. Chem.*, 2010, **20**, 7422.
- 24 Y. Li, F. Shen, H. Wang, F. He, Z. Xie, H. Zhang, Z. Wang, L. Liu, F. Li, M. Hanif, L. Ye and Y. Ma, *Chem. Mater.*, 2008, **20**, 7312.
- 10 25 S.-J. Yoon, J. W. Chung, J. Gierschner, K. S. Kim, M.-G. Choi, D. K. and S. Y. Park, *J. Am. Chem. Soc.*, 2010, **132**, 13675.
- 26 W. Huang, F. Tang, B. Li, J. Su and H. Tian, *J. Mater. Chem. C*, 2013, DOI: 10.1039/C3TC31913J26.
- 15 27 T. H. Xu, R. Lu, X. P. Qiu, X. L. Liu, P. C. Xue, C. H. Tan, C. Y. Bao and Y. Y. Zhao, *Eur. J. Org. Chem.*, 2006, 4014.
- 28 T. Xu, R. Lu, X. Liu, P. Chen, X. Qiu and Y. Zhao, *J. Org. Chem.*, 2008, **73**, 1809.
- 29 X. Qiu, R. Lu, H. Zhou, X. Zhang, T. Xu, X. Liu and Y. Zhao.
- 20 *Tetrahedron Lett.*, 2007, **48**, 7582.
- 30 J. A. Marsden, J. J. Miller, L. D. Shirtcliff and M. M. Haley, *J. Am. Chem. Soc.*, 2005, **127**, 2464.
- 31 J. Jia, K. Cao, P. Xue, Y. Zhang, H. Zhou and Ran Lu, *Tetrahedron*, 2012, **68**, 3626.
- 25 32 B. Li, Q. Li, B. Liu, Y. Yue and M. Yu, *Dyes Pigments*, 2011, **88**, 301.
- 33 H. Kotaka, G-i. Konishi and K. Mizuno, *Tetrahedron Lett.*, 2010, **51**, 181.
- 34 X. Y. Shen, W. Z. Yuan, Y. Liu, Q. Zhao, P. Lu, Y. Ma, I. D. Williams, A. Qin., J. Z. Sun and B. Z. Tang, *J. Phys. Chem. C*, 2012, **116**, 10541.
- 30 35 SHELXTL, Version 5.1; Siemens Industrial Automation, Inc. 1997; G. M. Sheldrick, SHELXS-97, Program for Crystal Structure Solution; University of Göttingen: Göttingen, 1997.